Calorimetry

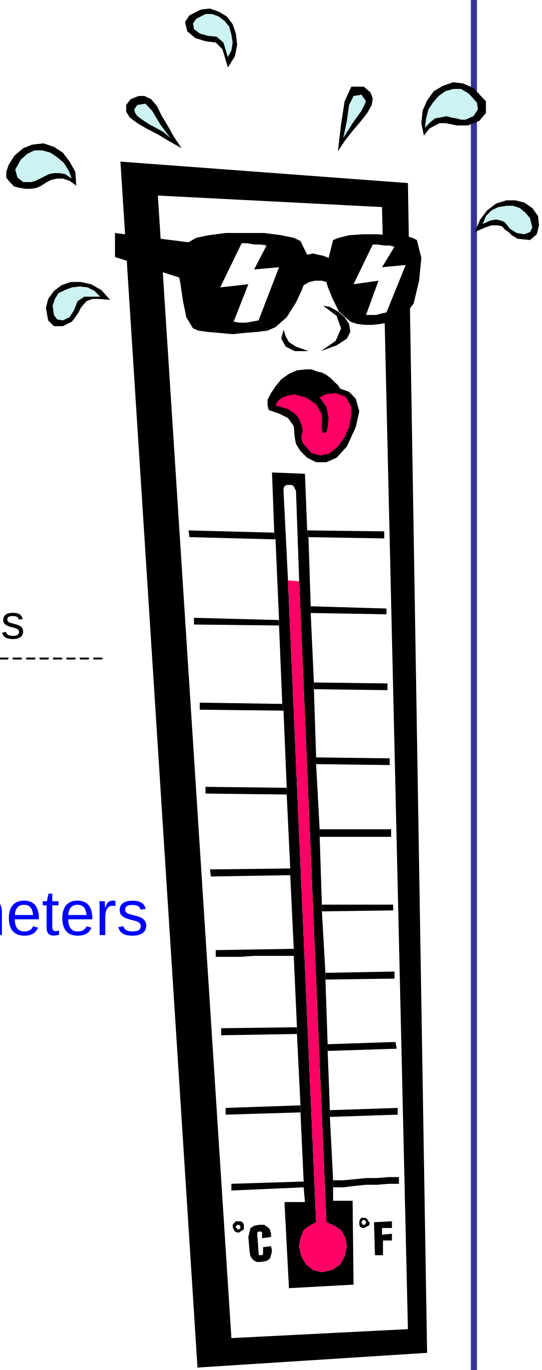

- **Basic principles**
  - Interaction of charged particles and photons
  - Electromagnetic cascades
  - Nuclear interactions
  - Hadronic cascades
- **Homogeneous calorimeters**
- **Sampling calorimeters**

- Calorimetry:

  Energy measurement by total absorption, combined with spatial reconstruction.

- Calorimetry is a "destructive" method

- Detector response $\propto$ E

- Calorimetry works both for
  - ⇨ charged ($e^{\pm}$ and hadrons)
  - ⇨ and neutral particles (n,γ)

- Basic mechanism: formation of
  - ⇨ electromagnetic
  - ⇨ or hadronic showers.

- Finally, the energy is converted into ionization or excitation of the matter.

Energy loss by Bremsstrahlung

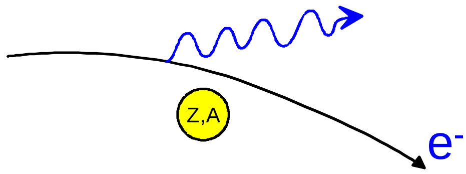

Radiation of real photons in the Coulomb field of the nuclei of the absorber

$$-\frac{dE}{dx} = 4\alpha N_A \frac{Z^2}{A} z^2 \left(\frac{1}{4\pi\varepsilon_0} \frac{e^2}{mc^2} \right)^2 E \ln \frac{183}{Z^{1/3}} \propto \frac{E}{m^2}$$

Effect plays a role only for e± and ultra-relativistic μ (>1000 GeV)

For electrons:

$$-\frac{dE}{dx} = 4\alpha N_A \frac{Z^2}{A} r_e^2 E \ln \frac{183}{Z^{1/3}}$$

$$-\frac{dE}{dx} = \frac{E}{X_0}$$

$$X_0 = \frac{A}{4\alpha N_A Z^2 r_e^2 \ln \frac{183}{Z^{1/3}}}$$

radiation length [g/cm²]

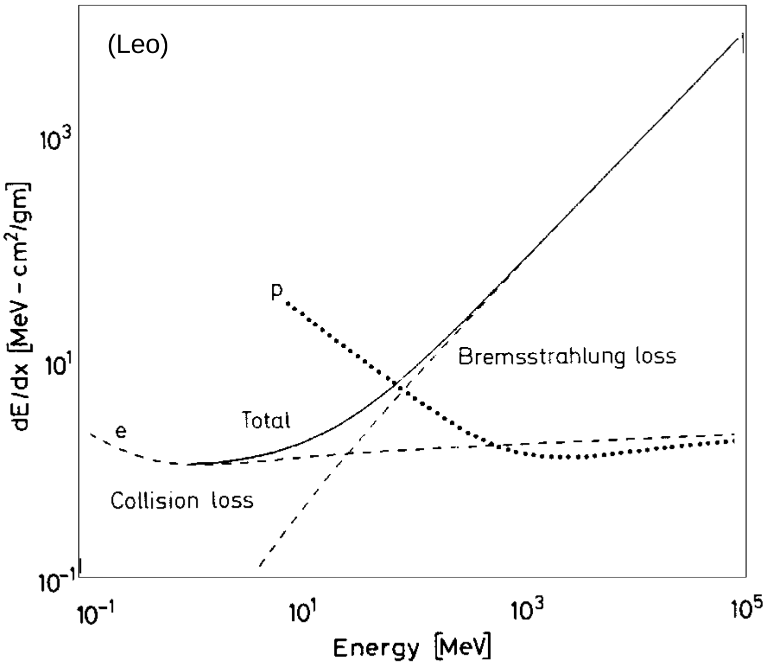

energy loss (radiative + ionization) of electrons and protons in copper

Critical energy E_c

$$\frac{dE}{dx}(E_c)\bigg|_{Brems} = \frac{dE}{dx}(E_c)\bigg|_{ion}$$

For electrons one finds approximately:

$$E_c^{solid+liq} = \frac{610 MeV}{Z+1.24} \qquad E_c^{gas} = \frac{710 MeV}{Z+1.24}$$

density effect of dE/dx(ionisation) !

$E_c(e^-)$ in Fe(Z=26) = 22.4 MeV

For muons

$$E_c \approx E_c^{elec}\left(\frac{m_m}{m_e}\right)^2$$

$E_c(\mu)$ in Fe(Z=26) $\approx$ 1 TeV

Interaction of photons

In order to be detected, a photon has to create charged particles and/or transfer energy to charged particles

- Photo-electric effect:

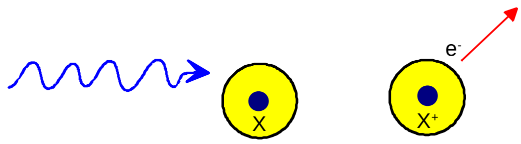

$$\gamma + \text{atom} \rightarrow \text{atom}^{+} + e^{-}$$

Only possible in the close neighborhood of a third collision partner $\rightarrow$ photo effect releases mainly electrons from the K-shell.

$$\sigma^{K}_{photo} = \left(\frac{32}{\varepsilon^{7}}\right)^{\frac{1}{2}} \alpha^{4} Z^{5} \sigma^{e}_{Th} \qquad \varepsilon = \frac{E_{\gamma}}{m_e c^2} \qquad \sigma^{e}_{Th} = \tfrac{8}{3}\pi r_e^2 \quad \text{(Thomson)}$$

Cross section shows strong modulation if $E_{\gamma} \approx E_{shell}$

At high energies ($\varepsilon \gg 1$)

$$\sigma^{K}_{photo} = 4\pi r_e^2 \alpha^{4} Z^{5} \frac{1}{\varepsilon}$$

$$\sigma_{photo} \propto Z^{5}$$

- Compton scattering:

$$g + e \rightarrow g' + e'$$

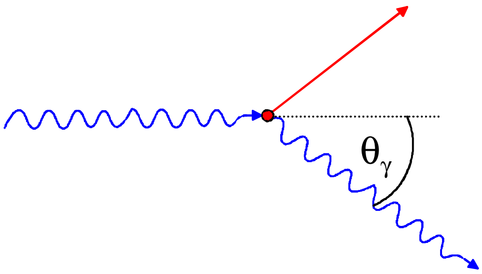

$$E'_g = E_g \frac{1}{1 + e\left(1 - \cos q_g\right)}$$

Assume electron as quasi-free.

Cross-section: Klein-Nishina formula, at high energies approximately $s_c^e \propto \frac{\ln e}{e}$

Atomic Compton cross-section: $s_c^{atomic} = Z \cdot s_c^e$

- Pair production

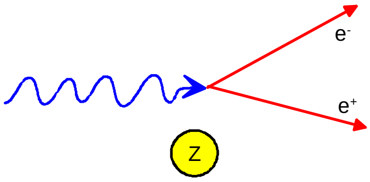

$$g + nucleus \rightarrow e^+e^- + nucleus$$

Only possible in the Coulomb field of a nucleus (or an electron) if $E_g \geq 2m_e c^2$

Cross-section (high energy approximation)

$$s_{pair} \approx 4ar_e^2 Z^2 \left(\frac{7}{9} \ln \frac{183}{Z^{\frac{1}{3}}} \right)$$

independent of energy !

$$\approx \frac{7}{9} \frac{A}{N_A} \frac{1}{X_0}$$

$$\approx \frac{A}{N_A} \frac{1}{l_{pair}}$$

$$l_{pair} = \frac{9}{7} X_0$$

Energy sharing between e^+ and e^- becomes asymmetric at high energies.

In summary: $I_g = I_0 e^{-mx}$ μ: mass attenuation coefficient

$$m = m_{photo} + m_{Compton} + m_{pair} + \ldots$$

$$m_i = \frac{N_A}{A} s_i \quad \left[cm^2 / g\right]$$

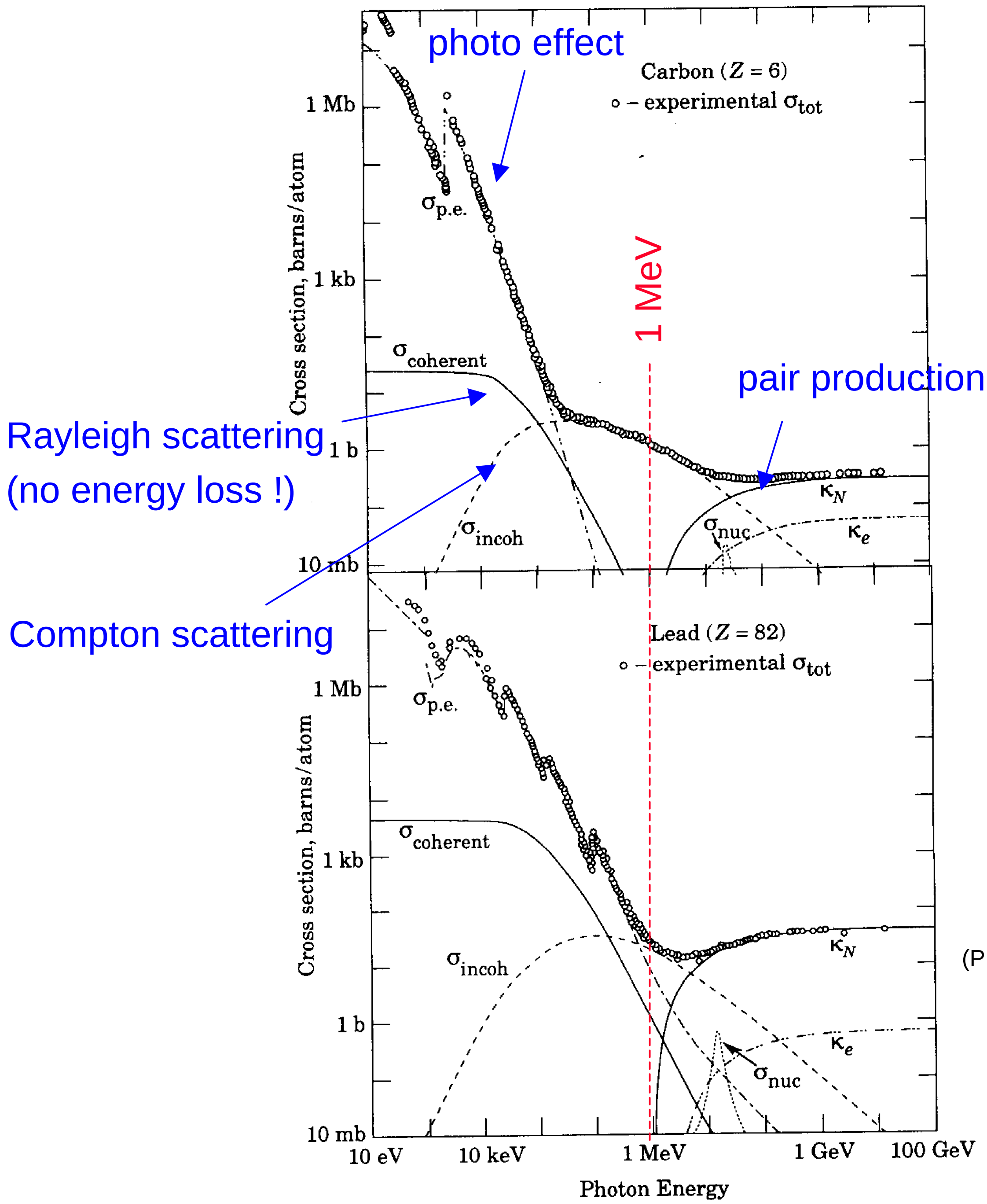

(PDG)

Reminder: basic electromagnetic interactions

e^+ / e^-

- Ionisation

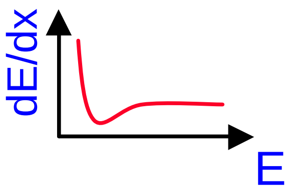

- Bremsstrahlung

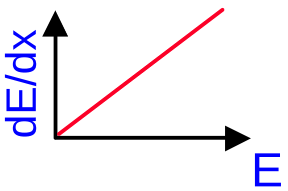

γ

- Photoelectric effect

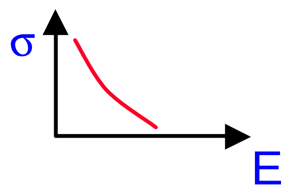

- Compton effect

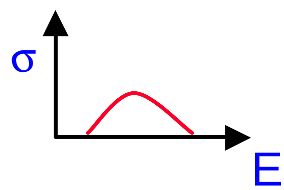

- Pair production

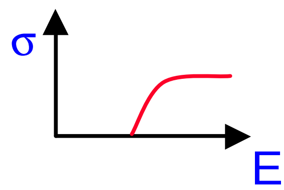

Electromagnetic Cascades (showers)

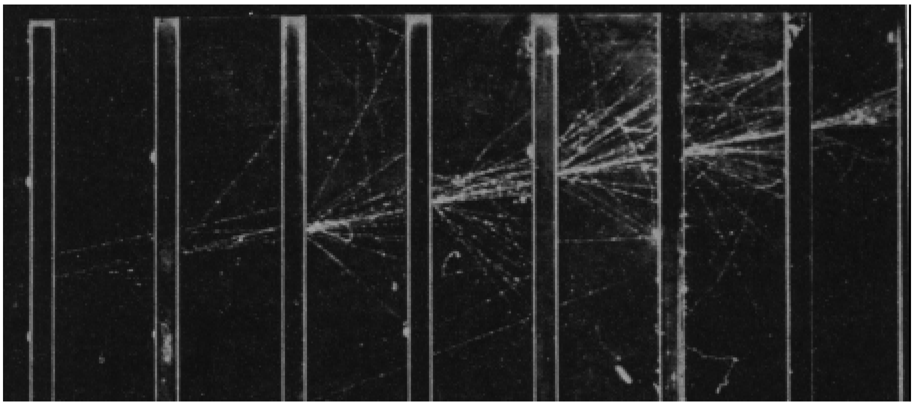

Electron shower in a cloud chamber with lead absorbers

Simple qualitative model

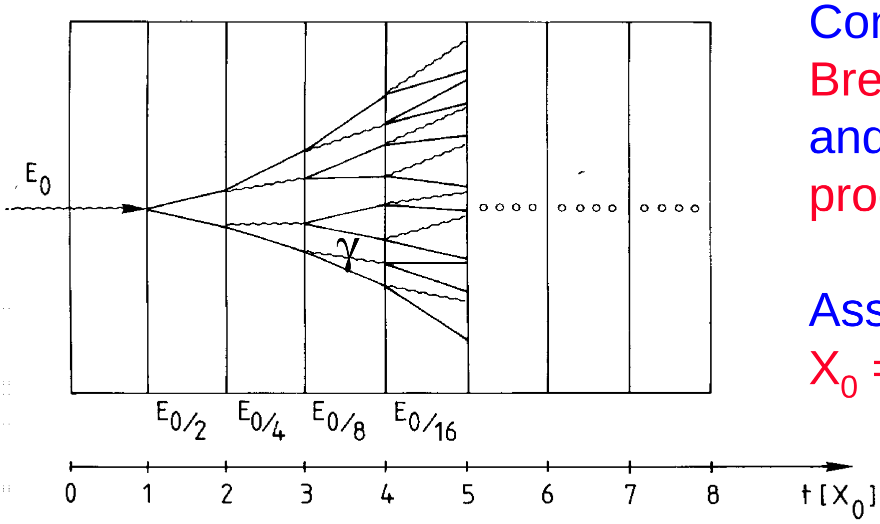

Consider only Bremsstrahlung and pair production.

Assume:
$X_0 = \lambda_{pair}$

$$N(t) = 2^t \qquad E(t)/\,particle = E_0 \cdot 2^{-t}$$

Process continues until $E(t) < E_c$

$$t_{\max} = \frac{\ln E_0/E_c}{\ln 2} \qquad N^{total} = \sum_{t=0}^{t_{\max}} 2^t = 2^{(t_{\max}+1)} - 1 \approx 2 \cdot 2^{t_{\max}} = 2\frac{E_0}{E_c}$$

After $t = t_{max}$ the dominating processes are ionization, Compton effect and photo effect → absorption.

Longitudinal shower development: $\frac{dE}{dt} \propto t^a e^{-t}$

Shower maximum at $t_{max} = \ln \frac{E_0}{E_c} \frac{1}{\ln 2}$

95% containment $t_{95\%} \approx t_{max} + 0.08Z + 9.6$

Size of a calorimeter grows only logarithmically with E_0

Transverse shower development: 95% of the shower cone is located in a cylinder with radius 2 R_M

$$R_M = \frac{21\,\text{MeV}}{E_c} X_0 \quad [g/cm^2]$$ Molière radius

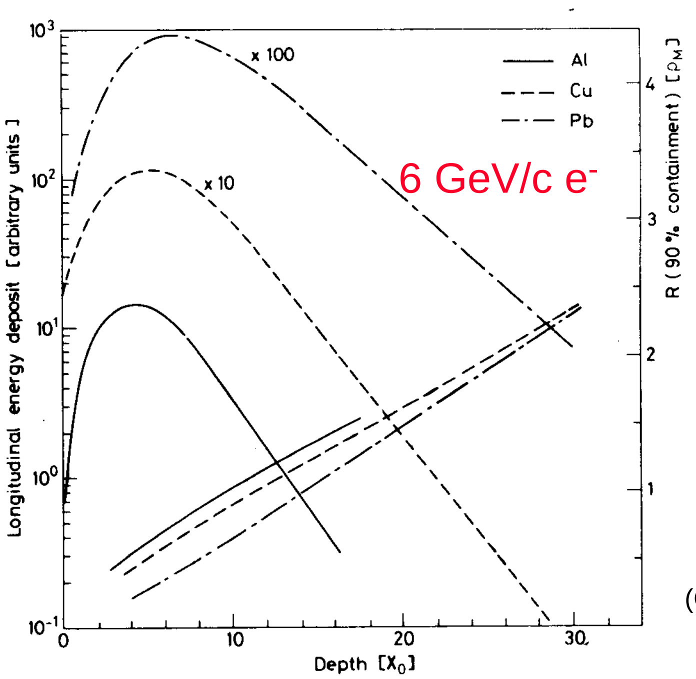

Longitudinal and transverse development scale with X_0, R_M

(C. Fabjan, T. Ludlam, CERN-EP/82-37)

Example: E_0 = 100 GeV in lead glass

E_c=11.8 MeV → $t_{max} \approx 13$, $t_{95\%} \approx 23$

$X_0 \approx 2$ cm, $R_M = 1.8 \cdot X_0 \approx 3.6$ cm

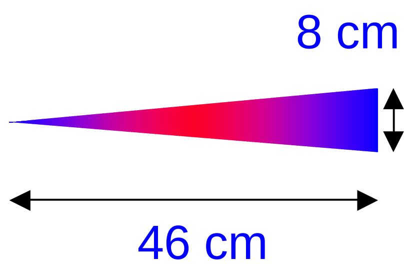

- Energy resolution of a calorimeter (intrinsic limit)

$$N^{total} \propto \frac{E_0}{E_c}$$

total number of track segments

$$\frac{s(E)}{E} \propto \frac{s(N)}{N} \propto \frac{1}{\sqrt{N}} \propto \frac{1}{\sqrt{E_0}}$$

holds also for hadron calorimeters

Also spatial and angular resolution scale like $1/\sqrt{E}$

Relative energy resolution of a calorimeter improves with E_0

More general:

$$\frac{s(E)}{E} = \frac{a}{\sqrt{E}} \oplus b \oplus \frac{c}{E}$$

Stochastic term

Constant term

Inhomogenities
Bad cell inter-calibration
Non-linearities

→ Quality factor !

Noise term

Electronic noise
radioactivity
pile up

Nuclear Interactions

The interaction of energetic hadrons (charged or neutral) is determined by inelastic nuclear processes.

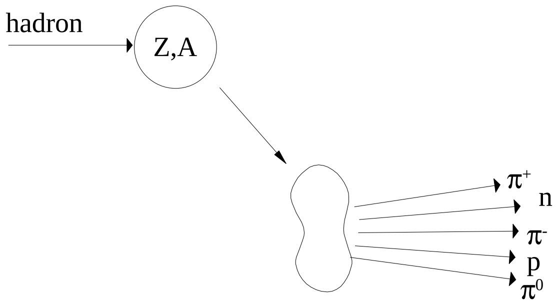

multiplicity $\propto$ ln(*E*)

p_t » 0.35 GeV/c

Excitation and finally breakup up nucleus → nucleus fragments + production of secondary particles.

For high energies (>1 GeV) the cross-sections depend only little on the energy and on the type of the incident particle (p, π, K…).

$$s_{inel} \approx s_0 A^{0.7} \qquad s_0 \approx 35\, mb$$

In analogy to X_0 a hadronic absorption length can be defined

$$l_a = \frac{A}{N_A s_{inel}} \propto A^{\frac{1}{4}} \quad \text{because} \quad s_{inel} \approx s_0 A^{0.7}$$

similarly a hadronic interaction length

$$l_I = \frac{A}{N_A s_{total}} \propto A^{\frac{1}{3}} \qquad l_I < l_a$$

Material	Z	A	ρ [g/cm³]	X_0 [g/cm²]	λ_a [g/cm²]
Hydrogen (gas)	1	1.01	0.0899 (g/l)	63	50.8
Helium (gas)	2	4.00	0.1786 (g/l)	94	65.1
Beryllium	4	9.01	1.848	65.19	75.2
Carbon	6	12.01	2.265	43	86.3
Nitrogen (gas)	7	14.01	1.25 (g/l)	38	87.8
Oxygen (gas)	8	16.00	1.428 (g/l)	34	91.0
Aluminium	13	26.98	2.7	24	106.4
Silicon	14	28.09	2.33	22	106.0
Iron	26	55.85	7.87	13.9	131.9
Copper	29	63.55	8.96	12.9	134.9
Tungsten	74	183.85	19.3	6.8	185.0
Lead	82	207.19	11.35	6.4	194.0
Uranium	92	238.03	18.95	6.0	199.0

For Z > 6: $\lambda_a > X_0$

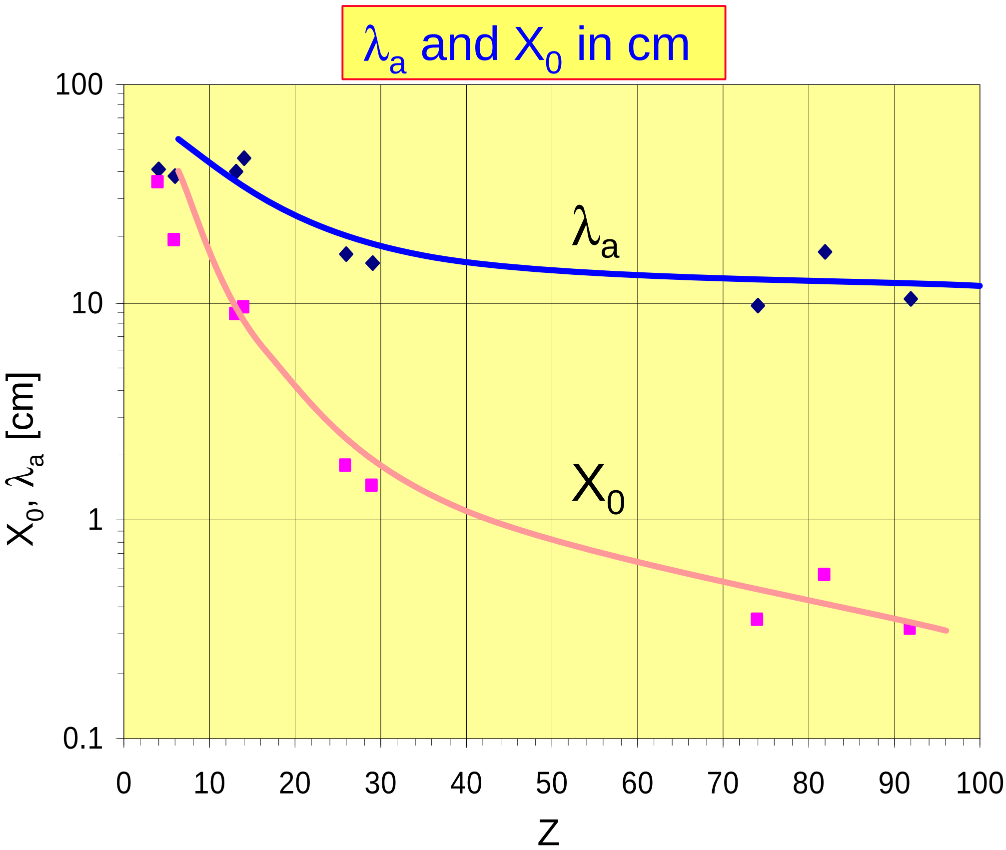

Interaction of neutrons

Neutrons have no charge, i.e. their interaction is based only on strong (and weak) nuclear force.

To detect neutrons, we have to create charged particles.

Possible neutron conversion and elastic reactions

- $n + {}^{6}Li \rightarrow \alpha + {}^{3}H$
- $n + {}^{10}B \rightarrow \alpha + {}^{7}Li$
- $n + {}^{3}He \rightarrow p + {}^{3}H$

$\Big\}$ $E_n < 20$ MeV

- $n + p \rightarrow n + p$ $\quad E_n < 1$ GeV

(H. Neuert, Kernphysikalische Messverfahren, G. Braun Verlag, 1966)

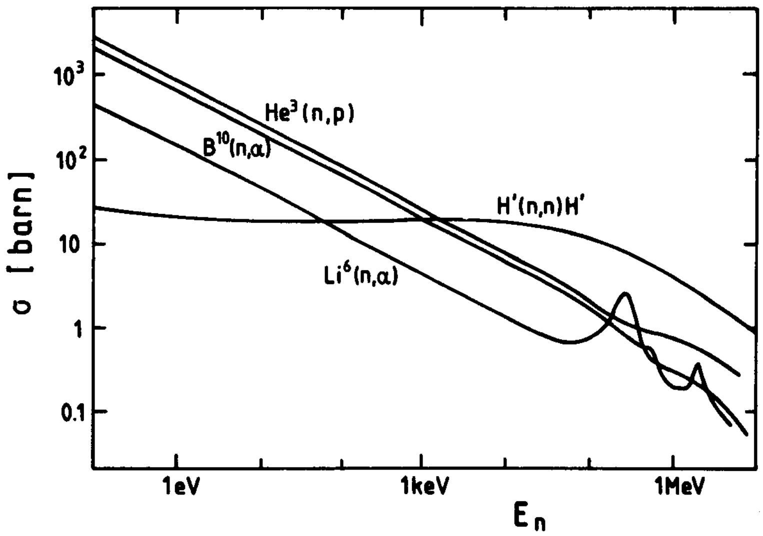

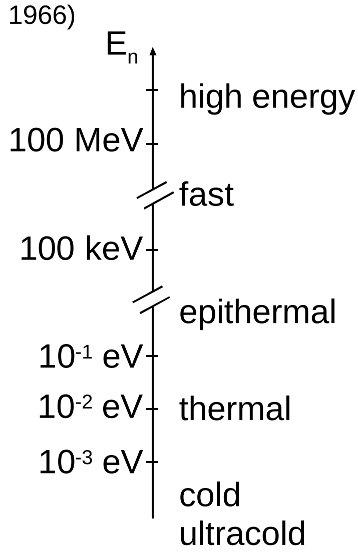

In addition there are

- neutron induced fission $\quad E_n \approx E_{th} \approx \frac{1}{40}$ eV
- hadronic cascades (see below) $\quad E_n > 1$ GeV

Interaction of neutrinos

Neutrinos interact only weakly ⟶ tiny cross-sections

For their detection we need again first a charged particle.

Possible detection reactions:

- $\nu_\ell + n \rightarrow \ell^- + p \qquad \ell = e, \mu, \tau$
- $\bar{n}_\ell + p \rightarrow \ell^+ + n \qquad \ell = e, \mu, \tau$

The cross-section for the reaction $\nu_e + n \rightarrow e^- + p$ is of the order of 10^{-43} cm^2 (per nucleon, $E_n \approx$ few MeV).

→ detection efficiency $e_{det} = s \cdot N^{surf} = s \cdot r \frac{N_A}{A} d$

1 m Iron: $e_{det} \approx 5 \cdot 10^{-17}$

Neutrino detection requires big and massive detectors (ktons) and high neutrino fluxes.

In collider experiments fully hermetic detectors allow to detect neutrinos indirectly:

- Sum up all visible energy and momentum.
- Attribute missing energy and momentum to neutrino.

example UA1: $W^+ \rightarrow e^+ + \nu_e$. Reconstruct transverse momentum of the ν_e from missing transverse momentum of the whole event.

Hadronic casacdes

Various processes involved. Much more complex than electromagnetic cascades.

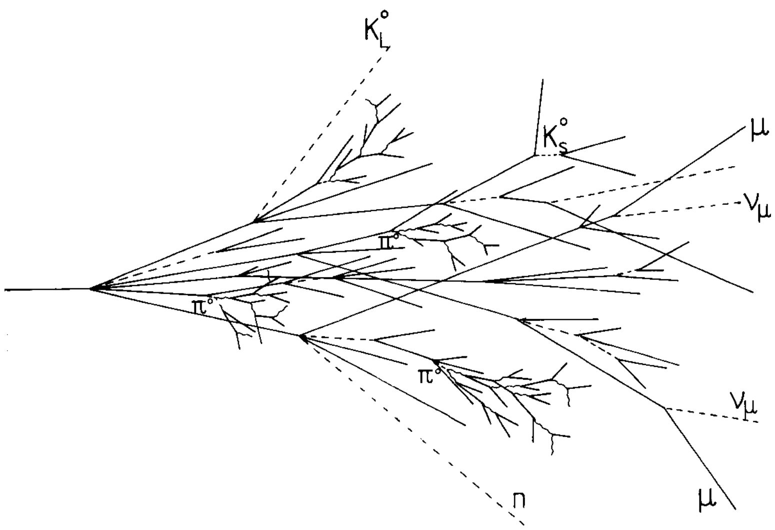

(Grupen)

Hadronic + electromagnetic component

↓

charged pions, protons, kaons ….
Breaking up of nuclei
(binding energy),
neutrons, neutrinos, soft γ's
muons …. → invisible energy

↓

neutral pions → 2γ →
electromagnetic cascade

$$n(p^0) \approx \ln E(GeV) - 4.6$$

example 100 GeV: $n(\pi^0) \approx 18$

Large energy fluctuations → limited energy resolution

Longitudinal shower development

$$t_{max}(l_I) \approx 0.2 \ln E[GeV] + 0.7$$

$$t_{95\%} \approx a \ln E + b$$

For Iron: a = 9.4, b=39
E =100 GeV
$\rightarrow t_{95\%} \approx$ 80 cm

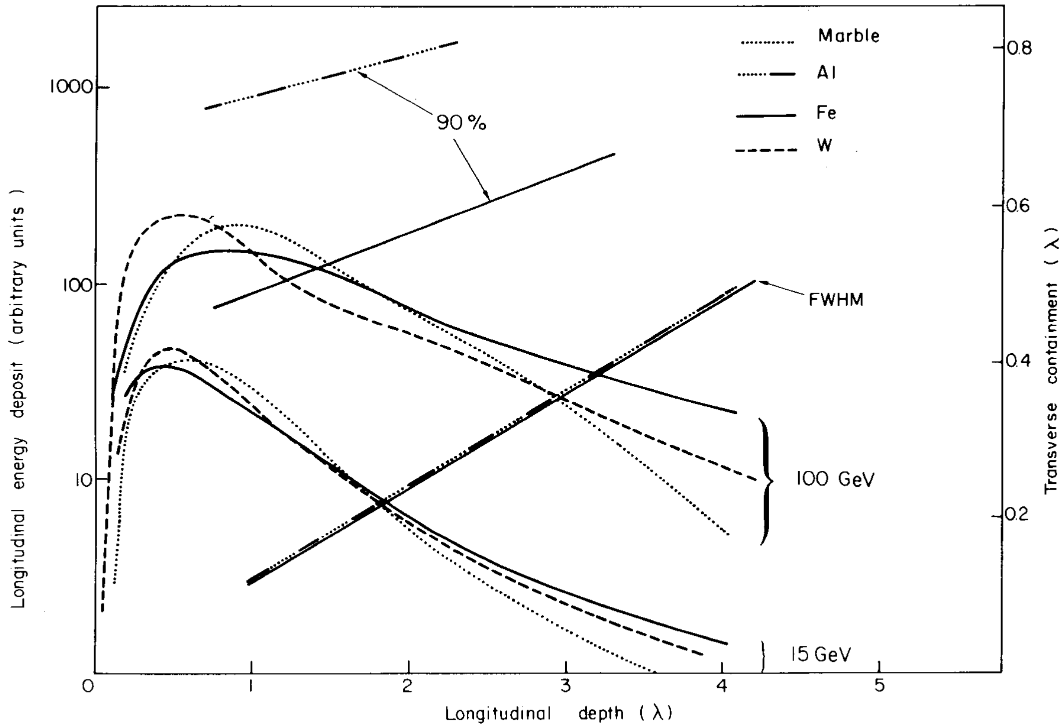

(C. Fabjan, T. Ludlam, CERN-EP/82-37)

Laterally shower consists of core + halo. 95% containment in a cylinder of radius λ_I.

Iron: λ_I =16.7 cm

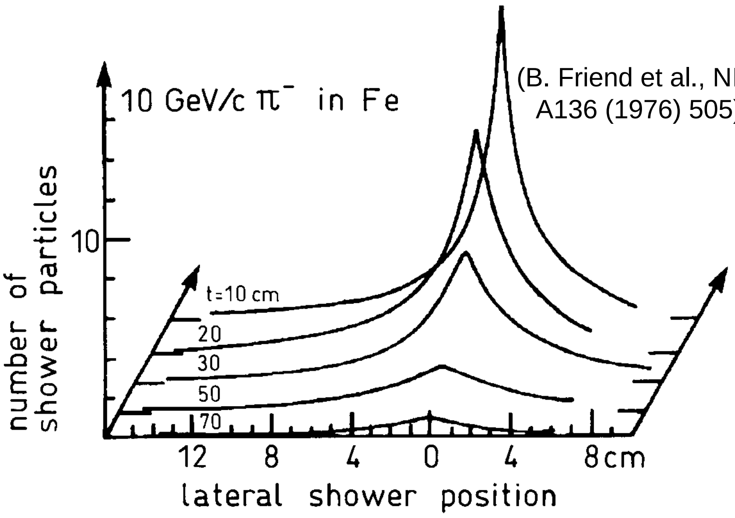

(B. Friend et al., NIM A136 (1976) 505)

Hadronic showers are much longer and broader than electromagnetic ones !

Material in front of calorimeter

Showers start in 'dead' material in front of calorimeter (other detectors, solenoid, support structure)

Install a highly segmented pre-shower detector in front of calorimeter

- recover lost energy
- improved background rejection due to good spatial resolution
- improve angular resolution

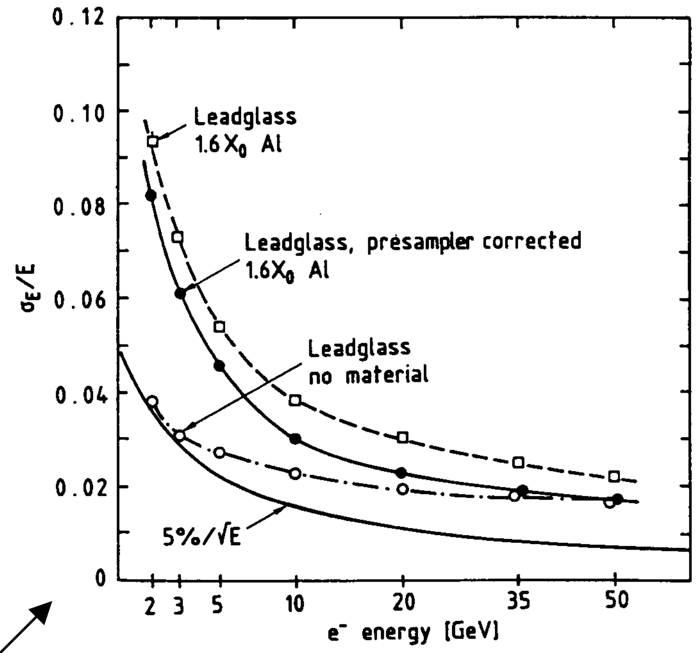

(C. Beard et al., NIM A 286 (1990) 117)

OPAL end cap calorimeter + pre-shower

Calorimeter types

- Homogeneous calorimeters:
  - ⇨ Detector = absorber
  - ⇨ good energy resolution
  - ⇨ limited spatial resolution (particularly in longitudinal direction)
  - ⇨ only used for electromagnetic calorimetry

- Sampling calorimeters:
  - ⇨ Detectors and absorber separated $\rightarrow$ only part of the energy is sampled.
  - ⇨ limited energy resolution
  - ⇨ good spatial resolution
  - ⇨ used both for electromagnetic and hadron calorimetry

Homogeneous calorimeters

Two main types: Scintillator crystals or "glass" blocks (Cherenkov radiation).

$\rightarrow$ photons. Readout via photomultiplier, -diode/triode

◆ Scintillators (crystals)

Scintillator	Density [g/cm^3]	X_0 [cm]	Light Yield γ/MeV (rel. yield)	τ_1 [ns]	λ_1 [nm]	Rad. Dam. [Gy]	Comments
NaI (Tl)	3.67	2.59	4×10^4	230	415	$\geq$10	hydroscopic, fragile
CsI (Tl)	4.51	1.86	5×10^4 (0.49)	1005	565	$\geq$10	Slightly hygroscopic
CSI pure	4.51	1.86	4×10^4 (0.04)	10 36	310 310	10^3	Slightly hygroscopic
BaF_2	4.87	2.03	10^4 (0.13)	0.6 620	220 310	10^5	
BGO	7.13	1.13	8×10^3	300	480	10	
$PbW0_4$	8.28	0.89	$\approx$100	10 10	$\approx$440 $\approx$530	10^4	light yield =f(T)

Relative light yield: rel. to NaI(Tl) readout with PM (bialkali PC)

◆ Cherenkov radiators

Material	Density [g/cm^3]	X_0 [cm]	n	Light yield [p.e./GeV] (rel. p.e.)	λ_{cut} [nm]	Rad. Dam. [Gy]	Comments
SF-5 Lead glass	4.08	2.54	1.67	600 (1.5×10^{-4})	350	10^2	
SF-6 Lead glass	5.20	1.69	1.81	900 (2.3×10^{-4})	350	10^2	
PbF_2	7.66	0.95	1.82	2000 (5×10^{-4})		10^3	Not available in quantity

Relative light yield: rel. to NaI(Tl) readout with PM (bialkali PC)

Examples

OPAL Barrel + end-cap: lead glass + pre-sampler

(OPAL collab. NIM A 305 (1991) 275)

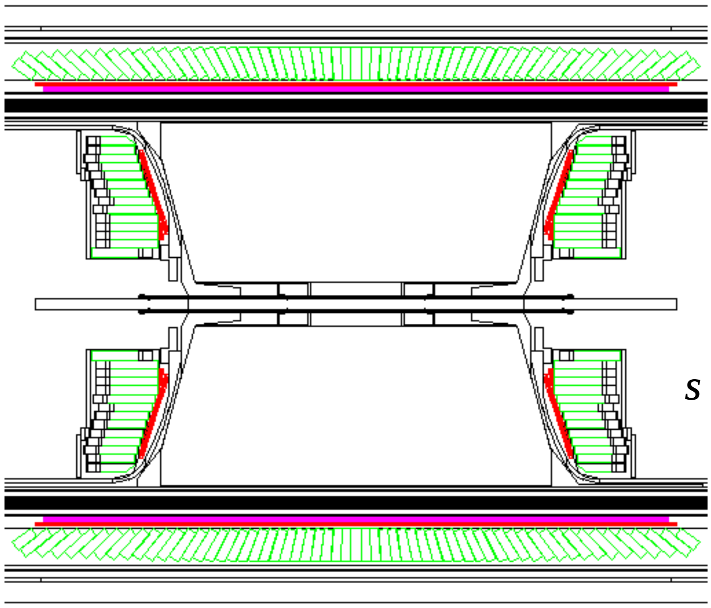

≈10500 blocks (10 x 10 x 37 cm^3, 24.6 X_0), PM (barrel) or PT (end-cap) readout.

$$s\,(E)/E = 0.06/\sqrt{E} \oplus 0.002$$

Spatial resolution (intrinsic) ≈ 11 mm at 6 GeV

BGO E.M. Calorimeter in L3

(L3 collab. NIM A 289 (1991) 53)

11000 crystals, 21.4 X_0,
temperature monitoring + control system
light output -1.55% / ºC

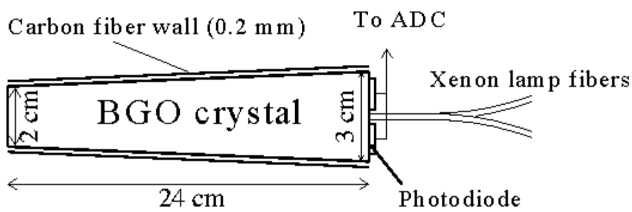

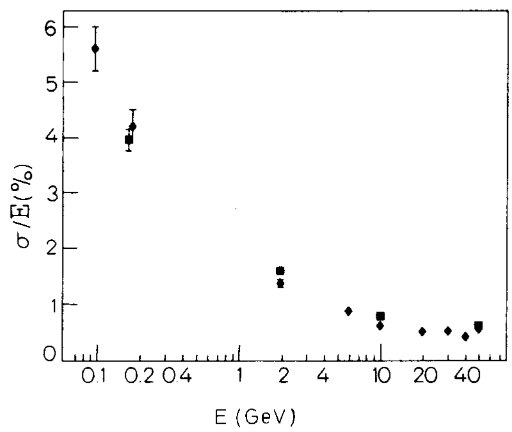

σ_E/E < 1% for E > 1 GeV
spatial resolution < 2 mm
(E >2 GeV)

Partly test beam results !

NA48: LKr Ionisation chamber (T = 120 K)

no metal absorbers → quasi homogenous !

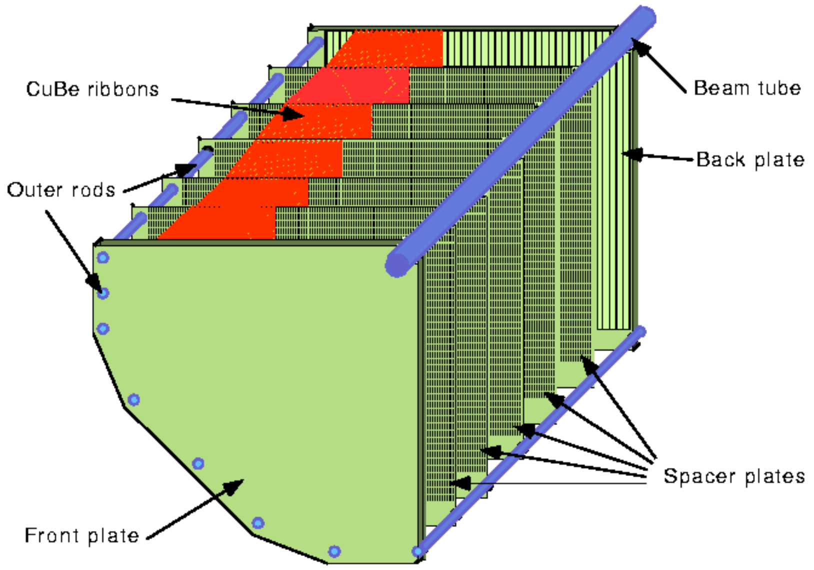

Cu-Be ribbon electrode

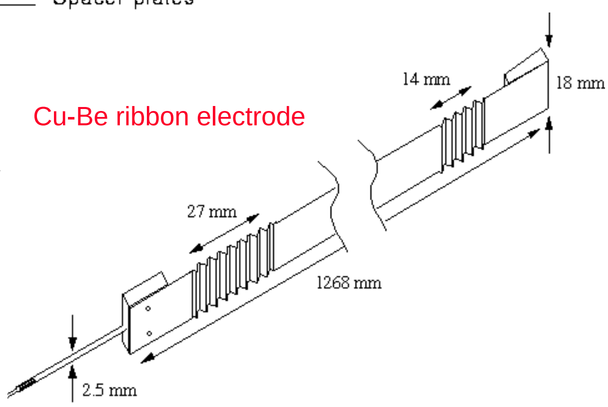

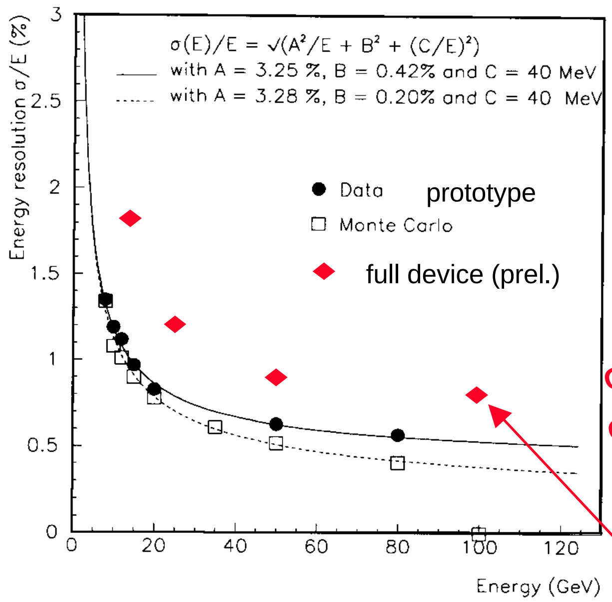

$\sigma_{x,y} \leq 1$ mm

$\sigma_t \approx 230$ ps

97 run: reduced performance due to problems with blocking capacitors → lower driftfield: 1.5 kV/cm rather than 5 kV/cm

(V. Marzulli, NIM A 384 (1996) 237,
M. Martini et al., VII International Conference on Calorimetry, Tuscon, 1997)

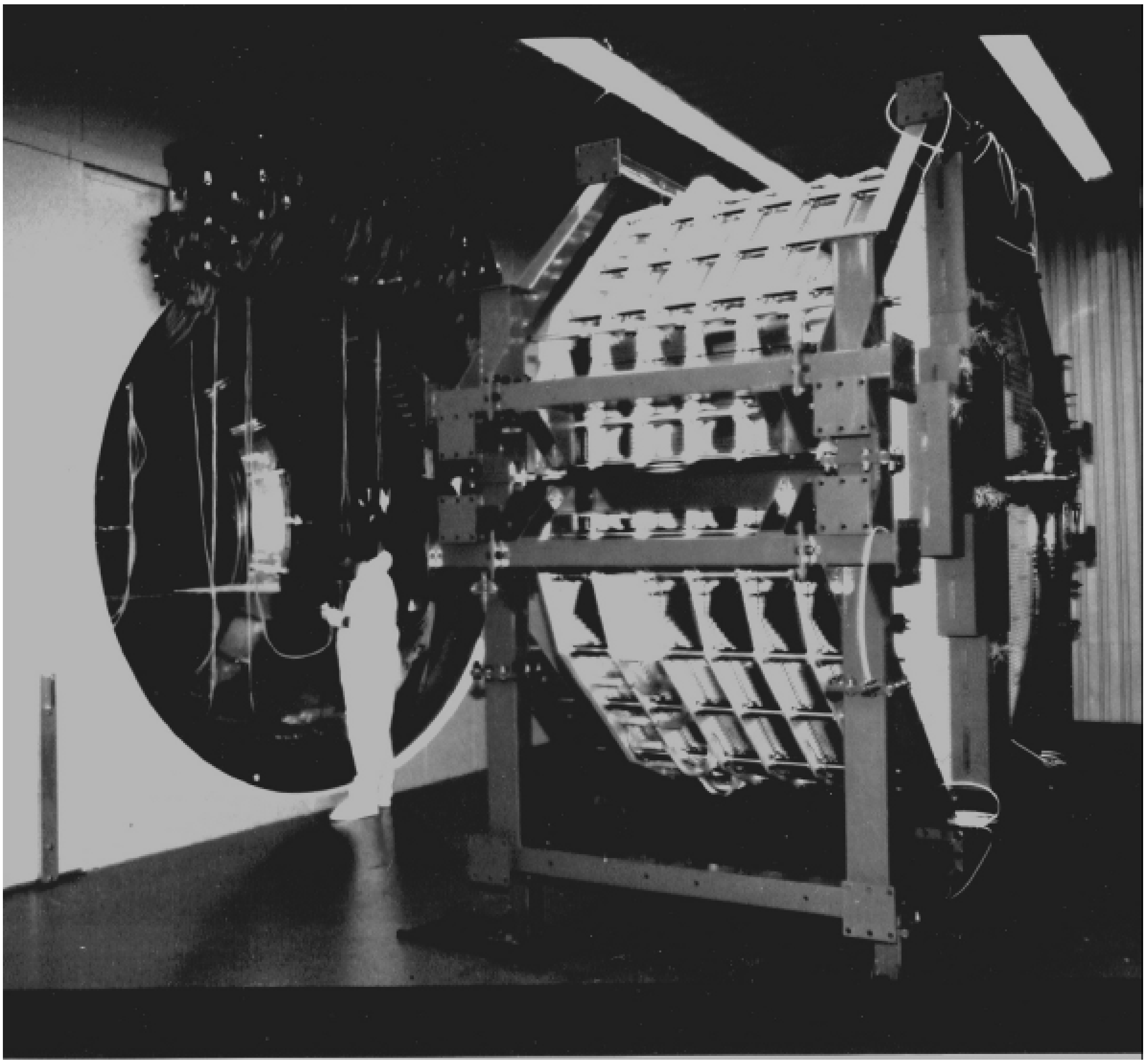

The NA48 LKr calorimeter prior to installation in the cryostat.

Homogeneous calorimeters

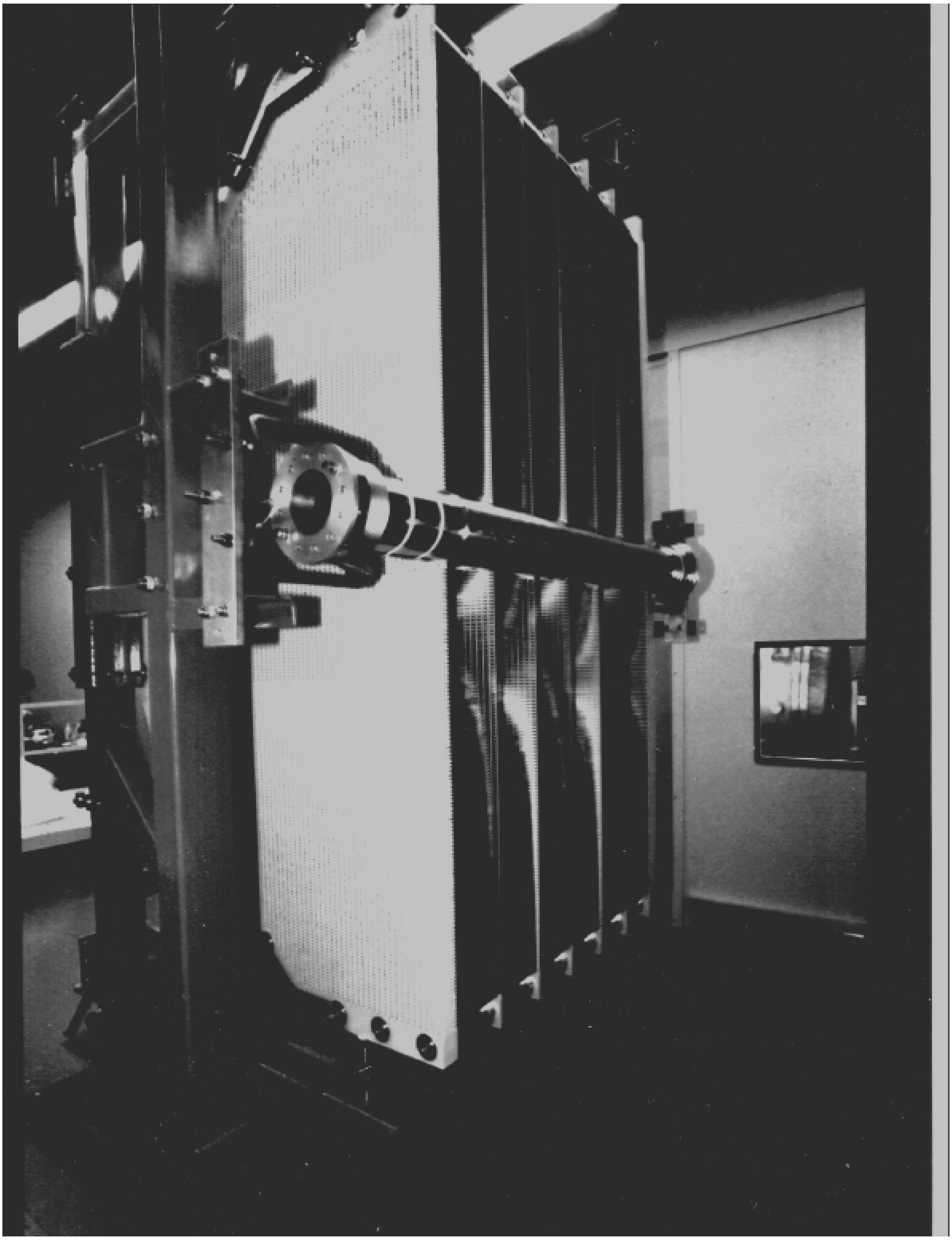

One half of the NA48 LKr calorimeter.

Sampling calorimeters

Absorber + detector separated → additional sampling fluctuations

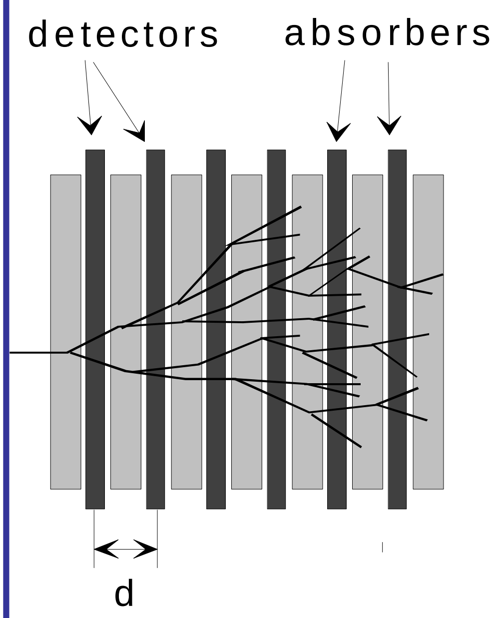

$$N = \frac{T_{\mathrm{det}}}{d}$$ Detectable track segments

$$= F(x)\frac{E}{E_c} X_0 \frac{1}{d}$$

$$\frac{\sigma(E)}{E} \propto \frac{\sqrt{N}}{N} \propto \sqrt{\frac{1}{E}} \cdot \sqrt{\frac{d}{X_0}}$$

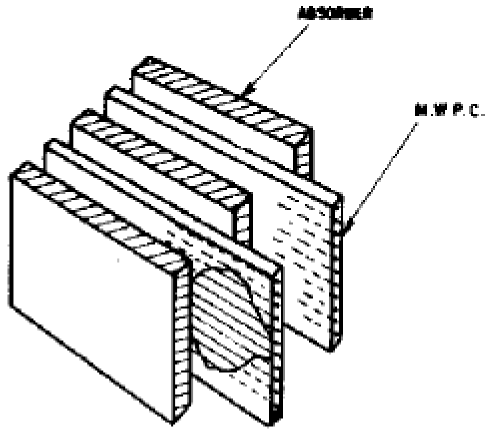

- MWPC, streamer tubes
- warm liquids
  - TMP = tetramethylpentane,
  - TMS = tetramethylsilane
- cryogenic noble gases:
  - mainly LAr (Lxe, LKr)
- scintillators, scintillation fibres, silicon detectors

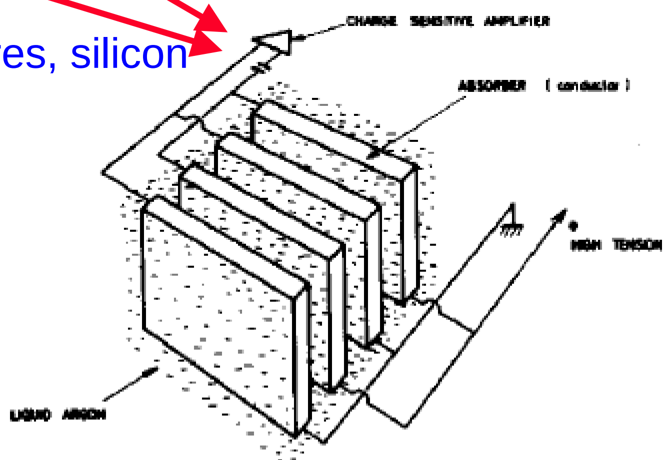

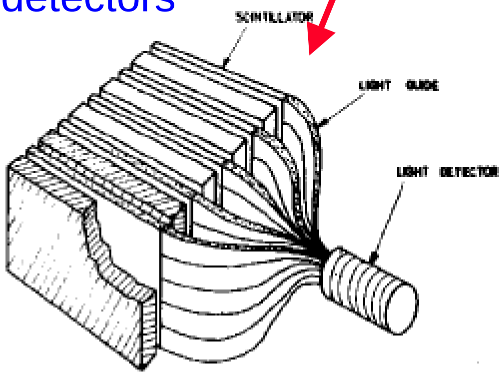

◆ ATLAS electromagnetic Calorimeter

Accordion geometry absorbers immersed in Liquid Argon

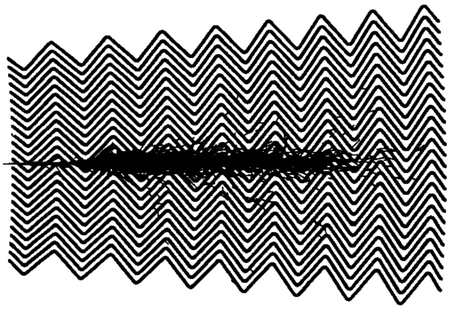

(RD3 / ATLAS)

Liquid Argon (90K)

+ lead-steal absorbers (1-2 mm)

+ multilayer copper-polyimide readout boards

→ Ionization chamber.

1 GeV E-deposit → 5 x10^6 e^-

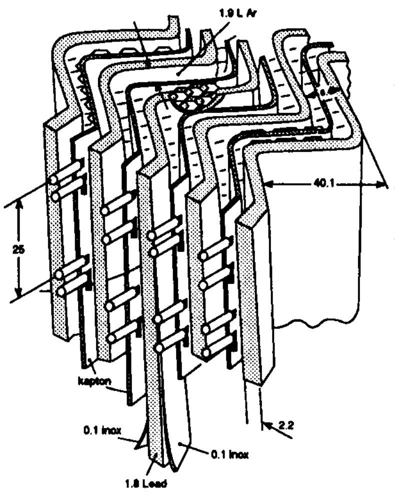

- Accordion geometry minimizes dead zones.
- Liquid Ar is intrinsically radiation hard.
- Readout board allows fine segmentation (azimuth, pseudo-rapidity and longitudinal) acc. to physics needs

Test beam results, e^- 300 GeV (ATLAS TDR)

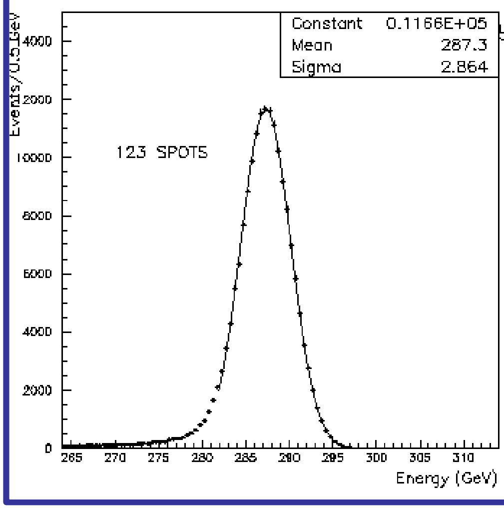

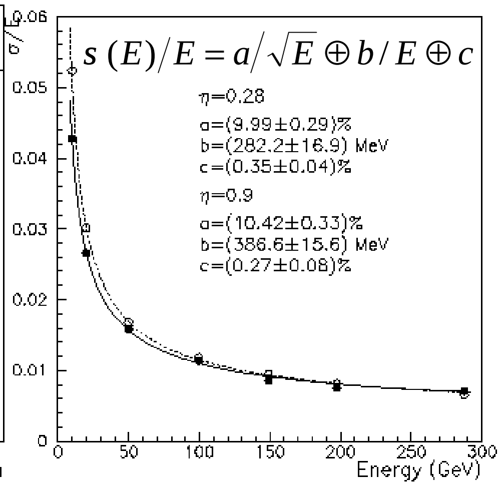

Spatial and angular uniformity ≈0.5%

Spatial resolution ≈ 5mm / $E^{1/2}$

CMS Hadron calorimter

Cu absorber + scintillators

↓

2 x 18 wedges (barrel)

+ 2 x 18 wedges (endcap) ≈ 1500 T absorber

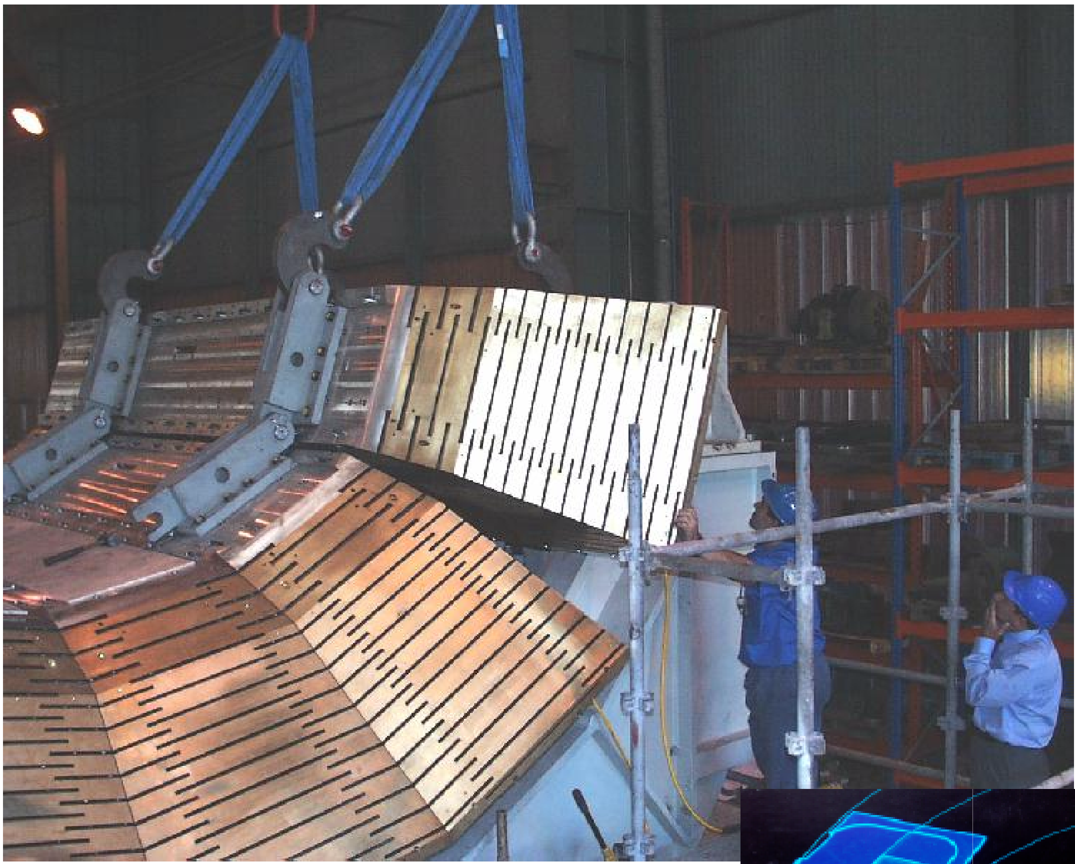

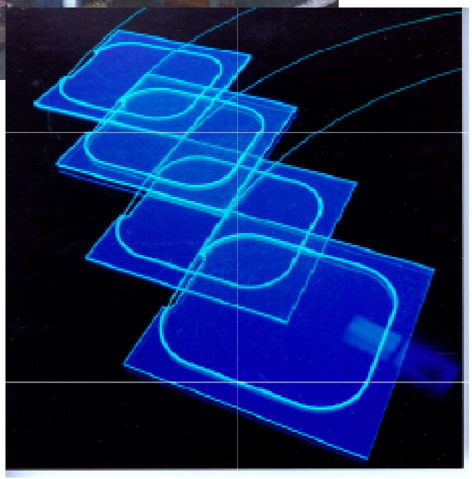

Scintillators fill slots and are read out via fibres by HPDs

Test beam resolution for single hadrons

$$\frac{\sigma_E}{E} = \frac{65\%}{\sqrt{E}} \oplus 5\%$$

4 scintillating tiles of the CMS Hadron calorimeter